

See discussions, stats, and author profiles for this publication at: <https://www.researchgate.net/publication/26678390>

Conformational Changes in a Flexible, Encapsulated Dicarboxylate: Evidence from Density Functional Theory Simulations

ARTICLE *in* THE JOURNAL OF PHYSICAL CHEMISTRY A · AUGUST 2009

Impact Factor: 2.69 · DOI: 10.1021/jp904556y · Source: PubMed

CITATIONS

3

READS

27

5 AUTHORS, INCLUDING:



Ali Kachmar

Pierre and Marie Curie University - Paris 6

21 PUBLICATIONS 154 CITATIONS

SEE PROFILE



Mauro Boero

Institut de Physique et Chimie des Matériaux

187 PUBLICATIONS 3,475 CITATIONS

SEE PROFILE

Conformational Changes in a Flexible, Encapsulated Dicarboxylate: Evidence from Density Functional Theory Simulations

Ali Kachmar,[†] Marc Bénard,^{*,†} Marie-Madeleine Rohmer,[†] Mauro Boero,^{‡,§} and Carlo Massobrio^{*,‡}

Laboratoire de Chimie Quantique, Institut de Chimie, UMR 7177 CNRS et Université de Strasbourg, 4, rue Blaise Pascal, F-67000 Strasbourg, France, Institut de Physique et Chimie des Matériaux de Strasbourg, UMR 7504 CNRS et Université de Strasbourg, 23 rue du Loess, F-67034 Strasbourg, France, and CREST, Japan Science and Technology Agency, 4-1-8 Honcho, Kawaguchi, Saitama 332-0012, Japan et JAIST, 1-1 Asahidai, Nomi-shi, Ishikawa 923-1292, Japan

Received: May 15, 2009; Revised Manuscript Received: June 30, 2009

The dynamical behavior of the $[\text{Mo}_{12}\text{O}_{12}\text{S}_{12}(\text{OH})_{12}\{\text{O}_2\text{C}-(\text{CH}_2)_n-\text{CO}_2\}]^{2-}$ complexes is analyzed via first-principles molecular dynamics simulations. Experimental X-ray data play the role of initial configurations for our search in the configuration space. We show that different stable and metastable conformers are possible, and these are thermally accessible at relatively low temperatures. This is the main outcome of our first-principles molecular dynamics approach in which the temperature allowing for thermal activation has been set to $T = 500$ K, which is consistent with the variable temperature ^1H NMR spectra of these complexes in solution taken at comparable, although moderately lower, temperature. This implies that a relatively large manifold of folding configurations is available to the encapsulated guest species. Moreover, the high flexibility of both the host cage and the inserted guests allows for the accommodation of a rather wide variety of functional groups with potential applications in several fields.

1. Introduction

Polyoxothiometalates (POTMs) represent a recent extension of the wide class of polyoxometalate inorganic compounds, which are at present recurrent in a wealth of applications covering a wide variety of fields, namely, catalysis, material synthesis, magnetism, nanoelectronics, self-assembly of metal oxide monolayers, protein crystallography, bleaching, medicine, and supramolecular chemistry.^{1,2} The emergence of the POTM family stems from the property of metal–metal bonded $[\text{M}_2\text{O}_2\text{S}_2(\text{H}_2\text{O})_6]^{2+}$ oxothioocations ($\text{M} = \text{Mo}^{\text{V}}, \text{W}^{\text{V}}$)^{3–5} to undergo self-condensation when templated with anionic precursors of appropriate size and shape. The host–guest complexes obtained from this process are made of a neutral, ring-shaped inorganic envelope with formula $[\text{Mo}_2\text{O}_2\text{S}_2(\text{OH})_2]_n$ resulting from the condensation of n cationic dimers ($n = 4–9$) and encapsulating one, and in some cases two, anionic species such as phosphate, metalate, or polycarboxylate molecules.^{6–9} The metal–metal bonds resulting from the coupling of the unique d-valence electron assigned to each Mo^{V} atom remain localized across the sulfido bridges. The $[\text{Mo}_2\text{O}_2\text{S}_2(\text{OH})_2]_n$ host rings are therefore organized as a series of n metal–metal bonded $(\text{MoO})_2(\mu\text{-S})_2$ moieties with short Mo–Mo distances (~ 2.8 Å) connected via double hydroxo bridges and long, nonbonded intermetallic distances (~ 3.3 Å).^{7–9} All complexes belonging to this family are therefore diamagnetic. Apart from the anionic species, an arbitrary number of water molecules may also be present inside the inorganic host; these H_2O monomers contribute to stabilize the complex via the formation of a rather strong hydrogen bond (H-bond) network with the guest anion(s).^{7,8}

The value of n is clearly driven by the minimal number of metal dimers that should be concatenated to confine the anion(s) with an acceptable strain on both species. Given these conditions, the inorganic ring becomes flexible enough to depart from its circular shape and to undergo distortions, in a nearly barrierless way, into an elliptic or more complicated structure.^{7–9} The factors that condition the stability of these supramolecular systems could be analyzed in more detail by comparing the relative stabilities in a relatively large series of dodecamolybdate $[\text{Mo}_{12}\text{O}_{12}\text{S}_{12}(\text{OH})_{12}]$ hosts encapsulating various types of di- and tricarboxylate guests. The number of carboxylate functional groups to be attached to the metal atoms is one of the key factors that makes the trimesate $[\text{C}_6\text{H}_3(\text{COO})_3]^{3-}$ guest a preferred structure in comparison with all dicarboxylate species. Beside this, a crucial factor for establishing the stability scale among the different dianionic complexes has been shown to be the mutual adaptability between the host and the guest, that is, the price to pay for the individual species to get adapted to the conformation they eventually adopt in the complex.^{8,9} The plasticity of the dodecamolybdenum host allows for a smooth accommodation of the guest, whose conformation does not significantly affect the host, and does not require the overcome of large activation barriers, unless the size of the guest becomes really unfit. Should these situations occur, the number n of concatenated metal dimers is modified accordingly. Therefore, a fundamental feature is the deformation of the guest anions. On one hand, those that are rigid because of aromatic or polyenic conjugation and are appropriately shaped to fit in the dodecamolybdenum cavity, such as terephthalate $[\text{C}_6\text{H}_4(\text{COO})_2]^{2-}$, tetramethylterephthalate $[\text{C}_6(\text{CH}_3)_4(\text{COO})_2]^{2-}$, and muconate $[\text{C}_4\text{H}_4(\text{COO})_2]^{2-}$, are able to enter the complex without undergoing any deformation and therefore rank highest in the stability hierarchy of $[\text{Mo}_{12}\text{O}_{12}\text{S}_{12}(\text{OH})_{12}(\text{dicarboxylate})]^{2-}$ complexes.⁸ On the other hand, some more flexible guest anions can induce

* Corresponding author. E-mail: benard@chimie.u-strasbg.fr.

[†] Institut de Chimie, UMR 7177 CNRS et Université de Strasbourg.

[‡] Institut de Physique et Chimie des Matériaux de Strasbourg, UMR 7504 CNRS et Université de Strasbourg.

[§] Japan Science and Technology Agency.

the formation of the same dodecamolybdenum host and get adapted to its structure. This is the case of the aliphatic dicarboxylates in which the two functional groups are connected with a linear chain of variable length composed of $N = 4$ to 6 methylene units. The price to pay for this versatility, at least for the pimelate ($N = 5$) and for the suberate ($N = 6$) guests, is the folding of the aliphatic chain and a clear loss of relative stability with respect to dodecamolybdate complexes. Dodecamolybdate complexes encapsulate either rigid guests or the adipate ($N = 4$) molecule, which fits into the inorganic host without undergoing any conformational change.^{8,9} The disorder of the suberate and pimelate molecules observed in the crystal structure of the corresponding complexes and the equilibrium between two conformations of different symmetries deduced from variable temperature ¹H NMR spectra for $[\text{Mo}_{12}\text{O}_{12}\text{S}_{12}(\text{OH})_{12}[\text{O}_2\text{C}-(\text{CH}_2)_5-\text{CO}_2]]^{2-}$ suggest that these guest molecules could undergo dynamical processes in solution.^{6a,9} In view of these stimulating hypotheses, it appears worthwhile to investigate the role of dynamics in determining the relative stability of the different conformers expected to exist for each of the above complexes. This can be accomplished through a search of equilibrium minima in the configuration phase space of each complex. This is the scope of the present work, in which the nature and the energetics of these processes are elucidated by means of first-principles molecular dynamics simulations.

2. Computational Methodology

For each complex $[\text{Mo}_{12}\text{O}_{12}\text{S}_{12}(\text{OH})_{12}[\text{O}_2\text{C}-(\text{CH}_2)_N-\text{CO}_2]]^{2-}$ ($N = 4, 5, 6$), simulations have been carried out within the Car–Parrinello molecular dynamics (CPMD) approach.^{10,11} The temperature was controlled by a standard velocity rescaling algorithm, and for the exchange and correlation functionals, we used a Becke¹² and Perdew¹³ generalized gradient approximation. The core–valence interaction was described by Troullier–Martins norm-conserving pseudopotentials;¹⁴ in the case of Mo, we used the semicore states 4s, 4p, and 4d, and for S, the 3d channel was included.¹⁵ A standard Kleinman–Bylander factorization was adopted for O, S, C, and H pseudopotentials,¹⁶ whereas a Gauss–Hermite quadrature formula turned out to be a more appropriate choice for Mo. Because of the presence of O atoms, whose wave functions are rapidly varying close to the nucleus and to the use of semicore states for Mo, our plane wave (PW) basis set was truncated at a relatively high energy cutoff of 70 Ry. In all dynamical simulations, a fictitious electronic mass of 200 au and a time step of 3.0 au (0.075 ps) ensured good control of the constants of motion.¹⁷

The complex was placed at the center of a cubic simulation cell of edge size $L = 23 \text{ \AA}$, which is sufficient for the charge density to be negligible on the cell ends, and periodic boundary conditions, typical of PW-based approaches, were released, thus simulating an isolated system, via the Barnett–Landman scheme.¹⁸ The starting geometry used for each complex was derived from the X-ray structure after solving the disorder problems by means of geometry optimizations carried out with the ADF software¹⁹ within the same Becke¹² and Perdew¹³ gradient-corrected DFT scheme used in the CPMD dynamical simulations. The structures were relaxed until residual forces on the atoms were less than 10^{-3} hartree/au. Several tests were performed to select the temperature most appropriate to the simulations. On one hand, a temperature of 700 K was shown to yield an irreversible decomposition of the complexes. On the other hand, a temperature lower than 400 K was not sufficient to overcome the energy barriers separating the various conformers (on the time scale of our simulations) and thus to

TABLE 1: Sequence of the C–C–C–C Torsion Angles (degrees) Deduced from the Geometries Associated with the Two Energy Minima Calculated with ADF Starting (i) from the Observed Experimental (ADF_{exp}) Structures and (ii) from the Energy Minima Obtained from CPMD Simulations (ADF_{CPMD})

	adipate		pimelate		suberate	
	ADF _{exp} ^a	ADF _{CPMD} ^b	ADF _{exp} ^a	ADF _{CPMD} ^b	ADF _{exp} ^a	ADF _{CPMD} ^b
C1–C2–C3–C4 ^c	179.9	–177.7	152.5	–85.7	–166.9	169.5
C2–C3–C4–C5	179.8	–62.2	81.8	–108.2	–55.3	72.0
C3–C4–C5–C6	179.9	–175.4	81.8	62.2	–56.6	–161.6
C4–C5–C6–C7			152.5	–170.9	179.2	70.3
C5–C6–C7–C8					114.0	174.3

^a Geometry optimized with ADF starting from the experimental crystal structure (Figure 1, upper panels). ^b Geometry optimized with ADF starting from the alternative geometry obtained from CPMD (Figure 1, lower panels). ^c Carbon atoms are numbered sequentially from top to bottom referring to the scheme of Figure 1.

induce the expected conformational changes into the encapsulated dicarboxylate structure. Finally, an average temperature of 500 K seems to represent a critical zone inside which the potential barriers can be crossed while maintaining the host–guest assembly.

All dynamical simulations started from the ADF-optimized stationary ground states. After an initial equilibration, the system was allowed to evolve for about 1.3 ps, and a velocity rescaling algorithm kept the temperature oscillating within the 500 ± 100 K range. Then, geometric configurations realized at the maxima of the temperature oscillations during the dynamics and corresponding to minima of the potential energy surface (PES) were selected, and the system was quenched down to 0 K by a standard annealing procedure. The equilibrium structures obtained in this way were then further optimized to relax also the electronic degrees of freedom. Whenever the system evolved toward a new minimum belonging to a PES basin different from the initial one (given by the experimental crystal structure), the new configuration of the complex was analyzed and further optimized via static DFT calculations within both a PW basis set approach (CPMD) and an atom-centered localized basis set approach (ADF) to check independently the stability of the new minima. The relative energies of the new basins, calculated with the CPMD and with the ADF approaches, respectively, are reported in the first two columns of Table 2. Apart from the energy difference with respect to the initial basin, the new minima present a distinctive folding of the carboxylate carbon chain, described by the sequence of the C–C–C–C torsion angles along the chain. A remarkable change in these torsion angles, obtained upon ADF optimization and reported in Table 1, indicates that a transition toward a different PES basin occurs. Further details will be given in the next section, whenever necessary to support the discussion.

In the static calculations and geometry optimizations carried out within the ADF approach, all atoms were described by the Slater basis sets referred to as TZP in the user’s guide.^{19c} The basis set for hydrogen is triple- ζ plus one p-type orbital. For nonmetal atoms, the core (He for oxygen, Ne for sulfur) is frozen and described by a single Slater function, whereas the valence set is triple- ζ and supplemented with a d-type polarization function. The small core (3s3p3d) of molybdenum was also modeled by a frozen Slater basis. The valence-shell is double- ζ for 4s, triple- ζ for 4p, 4d, and 5s, and supplemented with a single Slater orbital describing the 5p shell. The zero-order regular approximation (ZORA) has been used to model the scalar relativistic effects. Because the complexes are diamag-

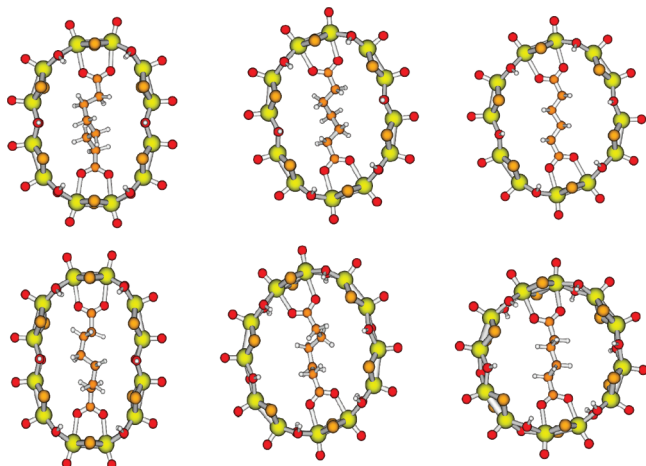


Figure 1. Structures of the $[\text{Mo}_{12}\text{O}_{12}\text{S}_{12}(\text{OH})_{12}\{\text{O}_2\text{C}-(\text{CH}_2)_N-\text{CO}_2\}]^{2-}$ complexes. Upper panels: structures derived from X-ray diffraction data and optimized via static DFT-based calculations. Lower panels: structures obtained after CPMD simulations at $500\text{ K} \pm 100\text{ K}$ and subsequent static relaxation. Guest = suberate ($N = 6$, left); pimelate ($N = 5$, center); adipate ($N = 4$, right).

netic, with localized Mo–Mo bonds and singlet ground states, all calculations were carried out with the restricted formalism.

3. Results and Discussion

The stable geometrical configuration of each of the $[\text{Mo}_{12}\text{O}_{12}\text{S}_{12}(\text{OH})_{12}\{\text{O}_2\text{C}-(\text{CH}_2)_N-\text{CO}_2\}]^{2-}$ complexes considered here was obtained by static optimization started from the corresponding structures observed from X-ray diffraction; these geometries are shown in the upper panels of Figure 1. In agreement with the observation, the structures encapsulating adipate ($N = 4$) and pimelate ($N = 5$) were assigned a C_2 symmetry during the optimization procedure. Conversely, the complex-encapsulating suberate, where the chain is longer and more flexible, was left unconstrained in the relaxation process. In each templated complex, the mutual adaptation between the host and the guest results in a more or less pronounced deformation of the host toward an elliptical shape and on the folding of the carboxylate carbon chain, defined by the sequence of its C–C–C–C torsion angles, reported in Table 1. In practice, the interplay between the flexibilities of both the host and the guest determines the final configuration of the complex.

The oxothiomolybdenum was found to be extremely flexible, and its global deformation from a circular to an elliptic shape occurred spontaneously during the simulations, indicating that these structural changes do not require the overcome of large activation energy barriers as long as the flattening of the ring does not induce any steric contact with the methylene groups. The only energetic cost for these deformations is due to local geometry variations induced by the coordination of the guest molecules and is essentially constant for all types of dicarboxylate ligands. On the contrary, the folding of the carbon chain has an energetic cost that increases with the number of CH_2 groups composing the chain.²⁰ We can then infer that this is responsible for the ordering of the relative stabilities of the complexes. Specifically, we observed a decrease in the stabilities of the three complexes as a function of the length of the carbon chain

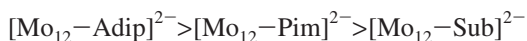


TABLE 2: Relative Energies of the Structures Found via First-Principles Molecular Dynamics and Subsequently Optimized within Plane-Wave (CPMD) and Localized Basis-Set (ADF) Approaches with Respect to the Minimum Associated with the Observed Configurations; Relative Energies of the Guest Carboxylate Molecules Assumed Isolated^{a,b}

	$E_{\text{rel}}(\text{Min})$ CPMD	$E_{\text{rel}}(\text{Min})$ ADF	E_{adjust} guest	E_{min} guest
$[\text{Mo}_{12}-\text{Adip}]^{2-}$	0 ^c +2.2	0 ^c +2.7	1.8 ^d 4.0	0 ^d 2.4
$[\text{Mo}_{12}-\text{Pim}]^{2-}$	0 +1.2	0 +2.5	8.6 12.1	6.7 6.6
$[\text{Mo}_{12}-\text{Sub}]^{2-}$	0 −3.5	0 −1.0	10.5 10.2	5.3 3.4

^a $E_{\text{adjust}}(\text{guest})$ corresponds to the relative energy, calculated using ADF, of the guest molecule assumed to be isolated with the geometry optimized in the complex. $E_{\text{min}}(\text{guest})$ corresponds to the relative energy optimized for the guest molecule assumed to be isolated starting from the geometry optimized in the complex. ^b For each complex, the upper line refers to the potential energy surface basin associated with the observed structure, and the lower line refers to the new basin obtained from the CPMD simulations. Energies are expressed in kilocalories per mole. ^c Values in this column refer to the minimum calculated for the considered complex starting from the observed structure. ^d Values in this column refer to the global minimum computed for the considered guest molecule, assumed isolated.

To rationalize these results, we performed a set of static relaxations, within the ADF approach, of the complex and of the guest alone, extracted from the complex after the optimization.

We can notice that the energy cost due to the deformation of the carboxylate guest can be expressed by two quantities, $E_{\text{min}}(\text{guest})$ and $E_{\text{adjust}}(\text{guest})$, both referring to relative ADF energies calculated with respect to the global minimum of the free guest molecule. $E_{\text{adjust}}(\text{guest})$ ²¹ refers to the energy obtained from a single-point calculation carried out on the carboxylate guest, using the atomic coordinates of the guest molecule obtained from a geometry optimization on the whole complex. If the same geometry is now used as a starting point for a geometry optimization of the guest molecule, then $E_{\text{min}}(\text{guest})$ corresponds to the relative energy of the obtained minimum. Therefore, (i) for a given starting geometry, $E_{\text{adjust}}(\text{guest})$ is always larger than $E_{\text{min}}(\text{guest})$, and (ii) $E_{\text{min}}(\text{guest})$ is strictly positive when the optimization process yields a local minimum; it is zero when optimization goes back to the global minimum. The latter case was obtained only with the smallest carboxylate (Adipate, $N = 4$), starting from the geometry optimized for $[\text{Mo}_{12}-\text{Adip}]^{2-}$ in the observed configuration (Table 2); $E_{\text{min}}(\text{Adip})$ is therefore zero, and $E_{\text{adjust}}(\text{Adip})$ remains very low (+1.8 kcal mol^{−1}, Table 2). The situation is different for the two other guests, pimelate and suberate, for which the geometry observed in the complex leads the free guests to energy basins associated with minima (E_{min}) located at +6.7 and +5.3 kcal mol^{−1}, respectively.

Models obtained by a set of molecular mechanics simulations,²² performed in our group, show that the number of such local minima compatible with the constraints required for an energetically favorable encapsulation inside the $\text{Mo}_{12}\text{O}_{12}\text{S}_{12}(\text{OH})_{12}$ ring, should be characterized by the following requirements:^{8,9} (i) an energy lower than ~ 10 kcal mol^{−1} above the global minimum; (ii) the coplanarity of the two carboxylate groups, and (iii) a distance between the carboxylate groups less than or similar to that observed in the X-ray structure. Within this framework, the number of possible local minima increases dramatically with the number of CH_2 groups comprising the

guest polymer chain because the longer the chain, the higher its flexibility and the number of conformations it can assume, even by simple thermal effects. It is therefore tempting to assign the increase in the average molecular symmetry with temperature deduced from variable temperature ^1H NMR studies to conformational changes affecting the guest carboxylate.

The unconstrained dynamical simulations were carried out at a target temperature of 500 ± 100 K, and, after equilibration, statistics were collected for 1.2, 2.6, and 2.6 ps for $[\text{Mo}_{12}\text{-Adip}]^{2-}$, $[\text{Mo}_{12}\text{-Pim}]^{2-}$, and $[\text{Mo}_{12}\text{-Sub}]^{2-}$, respectively. Although the temperature range used for the CPMD simulations is somewhat higher than that corresponding to the NMR experiments, the computed trajectories show that all three complexes can indeed undergo configuration changes of the guest molecule without involving any dissociation process. It should be stressed that the choice of a temperature larger than the one adopted in the experiments is fully legitimated by two sets of considerations. First, we have to cope with the time scale limitations of our molecular dynamics approach, in which the description of thermally activated events occurring experimentally at room temperature becomes possible provided that the actual simulation temperature is substantially larger. Indeed, working at a higher temperature can be considered to be the simplest “acceleration scheme” suitable to induce dynamical events hindered by insufficiently short temporal trajectories.²³ Second, temperatures used in simulations involving C- and O-made complexes have to be set at higher values with respect to experiments because of the approximations of both the functionals adopted and the numerical integration schemes.^{24,25} Because of its high flexibility, the oxothiomolybdate ring reacts first to the increase in temperature by slightly modifying its shape by either increasing the ellipticity, as occurs, for instance, in the case of $[\text{Mo}_{12}\text{-Sub}]^{2-}$, or by assuming a more circular shape, as in the case of $[\text{Mo}_{12}\text{-Pim}]^{2-}$, or even by reversing the ellipticity, that is, decreasing the major axis and increasing the minor axis, as observed in the case of $[\text{Mo}_{12}\text{-Adip}]^{2-}$. On a second stage, the guest carboxylate reacts either by an elongation of the carbon chain together with a partial decoordination, in the case of suberate, or by a contraction, for the two other guests, and eventually by changes in the chain conformation. The systems were subsequently cooled by a standard annealing procedure.

This confirmed that the final complexes found were new minima different from the starting ones. Finite temperature dynamics allowed for the crossing of activation energy barriers on the order of 1.0 to 2.0 kcal mol⁻¹, and the complexes relaxed toward new minima distinct from the ones given by the initial geometries. The value 1.0 to 2.0 kcal mol⁻¹ can be estimated by considering that 1 kcal amounts to $T = 500$ K (the average temperature of our simulations), and instantaneous configurations corresponding to statistical variations well above this target temperature cannot be ruled out. For each complex, these new minima have been characterized first at the CPMD¹¹ level after complete relaxation of the electronic and ionic degrees of freedom at 0 K and then further checked by performing static relaxations both within the PW basis-set approach and within the localized basis-set ADF code.¹⁹ The initial configurations and their related new minima are reported in Figure 1.²⁶ As mentioned, the folding of the carbon chains, characteristic of these new configurations, is defined by the sequence of their torsion angles, reported in Table 1 and compared with the corresponding torsion angles for the starting structures.

The relative energies of the new structures are quite similar when optimized either with CPMD, or with ADF, as expected.

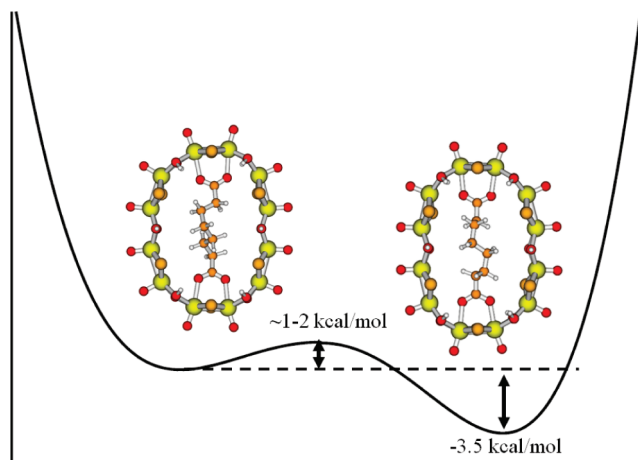


Figure 2. Structures and relative stabilities of the $[\text{Mo}_{12}\text{O}_{12}\text{S}_{12}(\text{OH})_{12}]\{\text{O}_2\text{C}(\text{CH}_2)_6\text{CO}_2\}^{2-}$ complexes. The lower minimum (-3.5 kcal mol⁻¹ according to the CPMD estimation) was obtained after dynamical simulations starting from the initial crystallographic structure.

They are slightly positive for $[\text{Mo}_{12}\text{-Adip}]^{2-}$ (+2.2 or +2.7 kcal mol⁻¹) and for $[\text{Mo}_{12}\text{-Pim}]^{2-}$ (+1.2 or +2.5 kcal mol⁻¹), respectively (Table 2). However, in the case of $[\text{Mo}_{12}\text{-Sub}]^{2-}$, the new minimum found by the CPMD dynamical exploration of the PES is located at lower energies (-3.5 kcal mol⁻¹) with respect to the initial (observed) structure (Figure 2). This result is confirmed by an ADF total energy calculation performed on this same structure, where the new configuration found turns out to be more stable than the initial one by 1.0 kcal mol⁻¹; these findings are reported in the first and second columns of Table 2, and, within the error bar typical of DFT calculation,²⁷ both results are in agreement and point to a preference for the system toward the newly found configuration. Care must be exercised when considering, for comparative purposes, the energies associated with the two minima shown in Figure 2 and the energy attributed to the transition state. The first two are the results of calculations on optimized geometries at $T = 0$ K, whereas the saddle barrier energy is an estimate based on the consideration of the average temperature imposed on the system ($T = 500$ K). Also, it has to be pointed out that the profile of the potential energy curve would feature, in the case of $[\text{Mo}_{12}\text{-Adip}]^{2-}$ and of $[\text{Mo}_{12}\text{-Pim}]^{2-}$, the first minimum on the left energetically lower than the second on the right, in a way that is compatible with the values of Table 2.

At variance with the case of adipate and pimelate guests, the conformation adopted by the suberate ligand in the new minimum is less hindered than the configuration corresponding to the initial observed structure, and this can account for its higher stability. We can remark that the suberate complex evolves from a nonsymmetric initial (observed) configuration to a symmetric one in the new minimum, as can also be deduced from the sequence of dihedral angles (Table 1), whereas the structures of adipate and pimelate shift from symmetric to nonsymmetric.

Conclusions

The present work has shown that guest dicarboxylates with flexible aliphatic framework can cross the PES barriers separating different folding configurations of the methylenic sequence by thermal activation. Without escaping or breaking the host envelope, the system can depart from the structure observed in the crystal and explore new minima of the PES associated with different possible folding configurations of the carbon chain

inside the envelope of the dodecamolybdate ring. The dynamic simulations have emphasized not only the flexibility of the guest molecule but also that of the inorganic host, and they have evidenced the existence of mutually adapted conformational changes of both the host and the guest components. In fact, when the temperature is raised to about 500 K, the [Mo₁₂] host is the quickest to respond by increasing, decreasing, or even inverting the elliptical deformation observed in the crystal structures of all [Mo₁₂O₁₂S₁₂(OH)₁₂{O₂C-(CH₂)_N-CO₂}]²⁻ complexes. These modifications of the host depend on the length of the methylene chain, and, in turn, the guest reacts so that the whole complex undergoes a synchronized movement of both moieties, making possible changes of the folding configuration of the carboxylate chains for all guests considered here. Specifically, the suberate guest (*N* = 6) is the one experiencing the most important conformational change, which is in agreement with its larger degrees of freedom for the chain folding. However, the aliphatic carboxylates with smaller *N* values, and especially for the adipate guest (*N* = 4), can also undergo modifications to fit better to the structure of the host.⁹

The dynamic behavior of the [Mo₁₂O₁₂S₁₂(OH)₁₂{O₂C-(CH₂)_N-CO₂}]²⁻ complexes, inspected via CPMD simulations, appears to be consistent with the previous interpretation of variable temperature ¹H NMR spectra of these complexes in solution. These NMR data indicate an evolution toward a high average symmetry for the complexes while increasing temperature from 215 to 340 K, and this was ascribed to intramolecular dynamic processes.⁹ It can then be inferred that a relatively large manifold of folding configurations is accessible to the encapsulated guest species, at least in the upper range of temperatures investigated. Although the multiplicity of the accessible configurations and the average structural symmetry along the dynamic pathway have not been experimentally verified yet, the computational evidence of at least one such structural change strengthens the hypothesis of a dynamic structural averaging at high temperature.

Acknowledgment. We acknowledge computational resources provided by CINES, IDRIS, and Centre d'Etudes du Calcul Parallèle et de la Visualisation of the University of Strasbourg. We are grateful to Fabien Muller and Romaric David for their technical assistance. We finally thank Sébastien Floquet and the group at the Institut Lavoisier (University of Versailles, France) for useful discussions throughout this work. The software VMD is used for the graphic presentation of the results.²⁸

Supporting Information Available: Complete sets of coordinates of the original starting structures and the new minima. This material is available free of charge via the Internet at <http://pubs.acs.org>.

References and Notes

- (1) (a) *Polyoxometalates: From Platonic Solids to Anti-Retroviral Activity*; Pope, M. T.; Müller, A., Eds.; Kluwer: Dordrecht, The Netherlands, 1994. (b) *Polyoxometalate Chemistry: From Topology via Self-Assembly to Applications*; Pope, M. T.; Müller, A., Eds.; Kluwer: Dordrecht, The Netherlands, 2001. (c) Long, D. L.; Burkholder, E.; Cronin, L. *Chem. Soc. Rev.* **2007**, *36*, 105. (d) *J. Mol. Catal. A: Chem.* **2002**, *179*, 1–242.
- (2) (a) Sartorel, A.; Carraro, M.; Scorrano, G.; De Zorzi, R.; Geremia, S.; McDaniel, N. D.; Bernhard, S.; Bonchio, M. *J. Am. Chem. Soc.* **2008**, *130*, 5006. (b) Khenkin, A. M.; Neumann, R. *J. Am. Chem. Soc.* **2008**, *130*, 14474. (c) Proust, A.; Thouvenot, R.; Gouzerh, P. *Chem. Commun.* **2008**, 1837. (d) Al Damen, M. A.; Clemente-Juan, J. M.; Coronado, E.; Martí-Gastaldo, C.; Gaita-Arino, A. *J. Am. Chem. Soc.* **2008**, *130*, 8874. (e) Mialane, P.; Dolbecq, A.; Sécheresse, F. *Chem. Commun.* **2006**, 3477. (f) Ogata, A.; Yanagie, H.; Ishikawa, E.; Morishita, Y.; Mitsui, S.; Yamashita, A.; Hasumi, K.; Takamoto, S.; Yamase, T.; Eriguchi, M. *Br. J. Cancer* **2008**, *98*, 399. (g) Wilson, E. F.; Abbas, H.; Duncombe, B. J.; Streb, C.; Long, D. L.; Cronin, L. *J. Am. Chem. Soc.* **2008**, *130*, 13876. (h) Mal, S. S.; Dickman, M. H.; Kortz, U.; Todea, A. M.; Merca, A.; Bogge, H.; Glaser, T.; Müller, A.; Nellutla, S.; Kaur, N.; van Tol, J.; Dalal, N. S.; Keita, B.; Nadjo, L. *Chem.—Eur. J.* **2008**, *14*, 1186.
- (3) (a) Miller, K. F.; Bruce, A. E.; Corbin, J. L.; Stiefel, E. I. *J. Am. Chem. Soc.* **1980**, *102*, 5102. (b) Coucouvanis, D.; Toupadakis, A.; Hadjikyriacou, A. *Inorg. Chem.* **1988**, *27*, 3272. (c) Sécheresse, F.; Cadot, E.; Simonet-Jegat, C. In *Metal Clusters in Chemistry*; Braunstein, P., Oro, L. A., Raithby, P. R., Eds.; Wiley-VCH: Weinheim, Germany, 1999; Vol. 1, pp 124–142.
- (4) Cadot, E.; Salignac, B.; Halut, S.; Sécheresse, F. *Angew. Chem., Int. Ed.* **1998**, *37*, 611.
- (5) Sécheresse, F.; Dolbecq, A.; Mialane, P.; Cadot, E. *C. R. Chim.* **2005**, *8*, 1927.
- (6) (a) Salignac, B.; Riedel, S.; Dolbecq, A.; Sécheresse, F.; Cadot, E. *J. Am. Chem. Soc.* **2000**, *122*, 10381. (b) Cadot, E.; Marrot, J.; Sécheresse, F. *Angew. Chem., Int. Ed.* **2001**, *40*, 774. (c) Cadot, E.; Sécheresse, F. *Chem. Commun.* **2002**, 2189. (d) Cadot, E.; Pouet, M. J.; Robert-Labarre, R.; du Peloux, C.; Marrot, J.; Sécheresse, F. *J. Am. Chem. Soc.* **2004**, *126*, 9127.
- (7) Lemonnier, J.-F.; Floquet, S.; Marrot, J.; Terazzi, E.; Piguet, C.; Lesot, P.; Pinto, A.; Cadot, E. *Chem.—Eur. J.* **2007**, *13*, 3548.
- (8) Lemonnier, J.-F.; Kachmar, A.; Floquet, S.; Marrot, J.; Rohmer, M.-M.; Bénard, M.; Cadot, E. *Dalton Trans.* **2008**, 4565.
- (9) Lemonnier, J.-F.; Floquet, S.; Kachmar, A.; Rohmer, M.-M.; Bénard, M.; Marrot, J.; Terazzi, E.; Piguet, C.; Cadot, E. *Dalton Trans.* **2007**, 3043.
- (10) Car, R.; Parrinello, M. *Phys. Rev. Lett.* **1985**, *55*, 2471.
- (11) CPMD; Copyright IBM Corp., 1990–2001; Copyright MPI für Festkörperforschung: Stuttgart, 1997–2004. <http://www.cpmd.org>.
- (12) Becke, A. D. *Phys. Rev. A* **1988**, *38*, 3098.
- (13) (a) Perdew, J. P. *Phys. Rev. B* **1986**, *33*, 8822. (b) Perdew, J. P. *Phys. Rev. B* **1986**, *34*, 7406.
- (14) Troullier, N.; Martins, J. L. *Phys. Rev. B* **1991**, *43*, 1993.
- (15) Rousseau, R.; Boero, M.; Bernasconi, M.; Parrinello, M.; Terakura, K. *Phys. Rev. Lett.* **1999**, *83*, 2218.
- (16) Kleinman, L.; Bylander, D. M. *Phys. Rev. Lett.* **1982**, *48*, 1425.
- (17) Schwegler, E.; Grossman, J. C.; Gygi, F.; Galli, G. *J. Chem. Phys.* **2004**, *121*, 5400.
- (18) Barnett, R. N.; Landman, U. *Phys. Rev. B* **1993**, *48*, 2081.
- (19) (a) te Velde, G.; Bickelhaupt, F. M.; Baerends, E. J.; Fonseca Guerra, C.; van Gisbergen, S. J. A.; Snijders, J. G.; Ziegler, T. *J. Comput. Chem.* **2001**, *22*, 931. (b) Fonseca Guerra, C.; Snijders, J.; te Velde, G.; Baerends, E. J. *Theor. Chem. Acc.* **1998**, *99*, 391. (c) *ADF2004.01*; SCM, Vrije Universiteit, Theoretical Chemistry: Amsterdam, The Netherlands; <http://www.scm.com>.
- (20) Boero, M.; Parrinello, M.; Terakura, K. *J. Am. Chem. Soc.* **1998**, *120*, 2746.
- (21) $E_{\text{adjust}}(\text{guest})$ corresponds to the relative energy of the guest molecule assumed to be isolated with the geometry optimized in the complex. $E_{\text{min}}(\text{guest})$ corresponds to the relative energy optimized for the guest molecule assumed to be isolated starting from the geometry optimized in the complex.
- (22) (a) SPARTAN, version 5.0; Wavefunction, Inc.: Irvine, CA. (b) Young, D. C. *Computational Chemistry: A Practical Guide for Applying Techniques to Real-World Problems*; Wiley-Interscience: New York, 2001.
- (23) Voter, A. F.; Montalenti, F.; Germann, T. C. *Annu. Rev. Mater. Res.* **2002**, *32*, 321–346.
- (24) Martyna, G. J.; Klein, M. L.; Tuckerman, M. J. *J. Chem. Phys.* **1992**, *97*, 2635.
- (25) Han, J.; Gee, R. H.; Boyd, R. H. *Macromolecules* **1994**, *27*, 7781.
- (26) The complete sets of coordinates of the original starting structures and the new minima are provided as Supporting Information.
- (27) Johnson, B. G.; Gill, P. M. W.; Pople, J. A. *J. Chem. Phys.* **1993**, *98*, 5612.
- (28) Humphrey, W.; Dalke, A.; Schulten, K. *J. Mol. Graphics* **1996**, *14*, 33. <http://www.ks.uiuc.edu/Research/vmd/>.

JP904556Y